J. Cell. Mol. Med. Vol 12, No 6B, 2008 pp. 2598-2608

Cytotoxic activity of nemorosone in neuroblastoma cells

D. Díaz-Carballo [a, *], S. Malak [b], W. Bardenheuer [b], M. Freistuehler [c], H. P. Reusch[a]

[a] Abteilung Klinische Pharmakologie, Ruhr-Universitaet Bochum, Bochum, Germany
[b] Universitaetsklinikum Essen, Innere Klinik, Tumorforschung, Essen, Germany
[c] Universitaetsklinikum Essen, Klinik fuer Augenheilkunde, Essen, Germany

Received: August 15, 2007; Accepted: January 3, 2008

Abstract

Neuroblastoma is the second most common solid tumour during childhood, characterized by rapid disease progression. Most children with metastasized neuroblastoma die despite intensive chemotherapy due to an intrinsic or acquired chemotherapy resistance. Thus, new therapeutic strategies are urgently needed. Here, we demonstrate that the novel compound nemorosone isolated from alcoholic extracts of *Clusia rosea* resins by reverse phase high pressure liquid chromatography (RP-HPLC) exerts cytotoxic activity in neuroblastoma cell lines both parental and their clones selected for resistance against adriamycin, cisplatin, etoposide or 5-fluorouracil. Cell cycle studies revealed that nemorosone induces an accumulation in G0/G1- with a reduction in S-phase population combined with a robust up-regulation of $p21^{Cip1}$. Furthermore, a dose-dependent apoptotic DNA laddering accompanied by an activation of caspase-3 activity was detected. Nemorosone induced a significant dephosphorylation of ERK1/2 in LAN-1 parental cells probably by the inhibition of its upstream kinase MEK1/2. No significant modulation of signal transducers JNK, p38 MAPK and Akt/PKB was detected. The enzymatic activity of immunoprecipitated Akt/PKB was strongly inhibited *in vitro*, suggesting that nemorosone exerts its anti-proliferative activity at least in part by targeting Akt/PKB in the cell lines studied. In addition, a synergistic effect with Raf-1 inhibitor BAY 43-9006 was found. Finally, nemorosone induced a considerable down-regulation of N-myc protein levels in parental LAN-1 and an etoposide resistant subline at the same drug-concentrations.

Keywords: nemorosone • *Clusia rosea* • neuroblastoma • cell cycle • apoptosis • isobologram • MYCN • Akt/PKB • ERK1/2

Introduction

Neuroblastoma originates from primitive neural crest cells and is the second most common solid tumour in childhood. The therapy of neuroblastoma is often hindered by chemotherapy resistance of the tumours, so that a large percentage of the patients die from metastasized neoplasia [1]. In the last years, several molecular markers for neuroblastoma have been identified, among which the expression of neurotrophin receptors, amplification and overexpression of the proto-oncogene MYCN, and other genetic alterations, such as deletions in the chromosomes 1p, 11q, 3p and partial gain of chromosome arm 17q (which is correlated with MYCN amplification) are considered to be the most reliable for assessment of tumour progression, aggressiveness and malignancy [2–6]. N-myc controls the transcription of more than 50 genes involved, amongst others, in cell proliferation, signal transduction, ribosome biogenesis, protein synthesis, apoptosis, cell cycle control and regulation of the cytoskeleton [7, 8]. An important cell cycle inhibitor negatively regulated by N-myc is $p21^{Cip1}$ Regulation of MYCN is mediated in part by glycogen synthase kinase (GSK)-3β, a component of the Wnt and Akt/PKB pathways [9, 10]. Other molecular markers for neuroblastoma malignancy include the neurotrophin receptors Tyrosine kinase (Trk) A, B and C which are responsible for survival, growth and differentiation of neural crest derived cells from the central nervous system. In neuroblastoma, the expression of Trk-A/Trk-C is associated with a favourable prognosis of the disease, whereas Trk-B is mainly expressed in aggressive neuroblastoma entities, being a prognostic marker for poor disease outcome. Signal transduction pathways controlled by neurotrophin receptors include the PI3K, phospholipase C (PLC)γ, Wnt/β-catenin, and the Ras/Raf/MEK/ERK1/2 MAPK pathways [11–13]. MEK1/2 are critical signal transducers at the intersection of several signal transduction pathways, which regulates cell

*Correspondence to: Dr. David Díaz-CARBALLO
Abteilung Klinische Pharmakologie, Ruhr-Universitaet Bochum,
Universitaetsstr. 150, 44801 Bochum, Germany.
Tel.: +49-234-32-28985
Fax: +49-234-32-14904
E-mail: david.diaz-carballo@rub.de

doi:10.1111/j.1582-4934.2008.00232.x

proliferation, survival, migration and differentiation as part of the Ras/Raf/MEK/ERK1/2 MAPK pathway. They can phosphorylate both ERK1/2 and GSK-3β. Activation of the ERK1/2 pathway is needed to block N-myc degradation, with MEK1/2 inhibitors consequently being likely candidates for the treatment of advanced neuroblastoma entities that are characterized by high expression of N-myc [14, 15].

In search for new therapeutic agents of natural origin, we have recently isolated a compound with strong cytotoxic activity from *Clusia rosea* flowers collected in Florida, USA. Analysis of its chemical structure showed that this molecule was previously published as nemorosone [16]. This compound showed cytotoxic activity *in vitro* against a panel of tumour cell lines including breast, colon, ovary, liver and lung carcinoma [17]. In order to elucidate the molecular mechanisms of neuroblastoma cells affected by nemorosone treatment, we investigated its influence on the cell cycle, the effects on topoisomerase and telomerase activities and the major regulatory proteins of different signal transduction pathways known to be important in neuroblastoma cells.

Materials and methods

Chemical isolation of nemorosone

Flowers of *Clusia sp.* are known for their abundant production of polyisoprenylated benzophenones [16]. We used flowers of *Clusia rosea* collected in Miami, Florida as source of nemorosone. Briefly, their resins were extracted in absolute ethanol for 10 days in the darkness at room temperature. The crude ethanolic extracts were desiccated and the dried product was re-suspended with a concentration of 100 mg/ml in methanol. Nemorosone was isolated from the methanolic extracts using sequential reverse phase high pressure liquid chromatography (RP-HPLC) techniques employing a Waters Separation Module Alliance 2690 HPLC system, detection was performed with a Waters 996 PDA detector, both controlled by the Millennium 4.0 Chromatography Manager software (Waters GmbH, Eschborn, Germany). Chemical fractionation was performed on a 250 × 21 mm semi-preparative column packed with Nucleosil 100-7 C18 (Macherey-Nagel, Dueren, Germany) at a controlled temperature of 40°C, using a gradient system starting at time point zero with a mixture of ammonium formiate (0.01 M, pH 7.0), methanol and acetonitrile [(50:30:20) (v/v/v)]. The composition of this mixture changed linearly within 210 min. to methanol:acetonitrile = 80:20 (v/v) at a flow rate of 4 ml/min. The purity (98% HPLC) of nemorosone was further analysed employing a Symmetry C18 column of 150 × 2.1 mm (Waters GmbH, Eschborn, Germany) using the same chromatographic conditions as described above at a flow rate of 0.5 ml/min.

Cell culture and determination of IC50 values

Two NB cell lines were chosen based on differences in their molecular biology. LAN-1 parental cell line (henceforth referred to as LAN-1) displays high amplification of MYCN and is highly invasive. In contrast, NB69 has no MYCN amplification and displays low invasiveness. Additionally, both cell lines differentially express neuron-specific Enolase (NSE) tumour marker. Furthermore, two non-tumoural cell lines were included in the study as controls.

With the aim of determining the IC_{50} of nemorosone, the Sulforhodamine B (SRB) proliferation assay was performed [18]. Cytotoxicity was analysed at concentrations ranging from 1 to 40 μM of this drug after 24 hrs of drug exposition. IC_{50} values were interpolated from semi-logarithmic dose-response plots.

Generation of cell lines resistant to chemotherapeutic agents

Acquired resistance to cytostatics was developed in LAN-1 by exposing cell cultures to increasing drug levels. Briefly, IC_{50} values for adriamycin, cisplatin, etoposide and 5FU were determined in LAN-1 by SRB assay. Exponentially growing cells were then exposed to 2-fold the IC_{50} for 24 hrs. For recovery, cells were washed and incubated with drug-free culture medium until new colonies had formed. This procedure was repeated several times, each time doubling the original IC_{50} up until 64-fold the IC_{50} was reached. The surviving cells were subjected to a resistance selection by incubation with increasing concentrations of the respective drugs (16- to 512-fold the IC_{50}) for 24 hrs. Cells which proliferated at higher drug concentrations (cisplatin 32-fold, etoposide and adriamycin 128-fold, and 5FU 64-fold) within one week were considered chemotherapy refractory. These resistant colonies were maintained in continuous presence of the respective drug at 10-fold the original IC_{50}. Thereafter, the resistance factor (RF) was determined as new IC_{50}/original IC_{50}. The expression of multiple drug resistance (MDR)1 was measured by fluorescence activated cell sorting (FACS) using anti-MDR1 monoclonal antibody (Novus Biologicals, Littleton, CO, USA) and represented as % of MDR1-expressing cells in relation to the parental (Table 1).

Cell cycle analysis

Cell cycle analyses were performed employing FACS, combining propidium iodide (PI, Sigma-Aldrich, Munich, Germany) staining and 5-bromo-2'-deoxyuridine (BrdU, Sigma-Aldrich, Munich, Germany) incorporation as described by Tsugita [19]. 1×10^6 LAN-1 cells in exponential growth phase were incubated with 8 μM of nemorosone for 24 hrs (end-point). Anti-BrdU FITC-conjugated mAb was purchased from Pharmingen (Heidelberg, Germany). BrdU incorporation and DNA content were measured using an EPICS XL flow cytometer (Beckman Coulter, Krefeld, Germany) at an excitation of λ = 488 nm.

Western Blot analysis

5×10^6 LAN-1 cells in exponential growth phase were incubated with increasing concentrations (4–12 μM) of nemorosone for 24 hrs. Cells were then washed with cold PBS, centrifuged and pellets were lysed in RIPA buffer (150 mM NaCl, 1 mM ethylenediaminetetraacetic acid [EDTA], 1% Triton x-100, 1% sodium deoxycholate, 0.1% SDS, 50 mM Tris-HCl pH 7.4) in the presence of a proteinase inhibitor cocktail according to the manufacturer's instructions (Roche Diagnostics GmbH, Mannheim, Germany) for 30 min. on ice and then subsequently centrifuged at 14.000 × g at 4°C

Table 1 *In vitro* cytotoxicity of nemorosone in neuroblastoma and fibroblasts cell lines. Cytotoxicity of nemorosone over 24 hrs in a panel of tumour (both parental and chemotherapy refractory) and non-tumour cell lines as assessed by Sulforhodamine B (SRB) assay. Values represent the means ± standard deviation of at least three independent experiments. RF, resistance factor: (IC50 resistant/ IC_{50} parental). Parental and chemotherapy refractory sub-lines were employed. (MDR1: multi-drug resistance 1, was determined by FACS and represented in %) No cross-resistance was observed. Fibroblasts were less sensitive to nemorosone.

Cell Lines	Histology	Resistant against	Resistance factor	IC50 nemorosone (μM)
LAN-1* MDR1-	Neuroblastoma	-	1	4.10±0.28
LAN-1 CP*	Neuroblastoma	Cisplatinum	32	4. 22±0.26
LAN-1 ETO* >99 % MDR1+	Neuroblastoma	Etoposide	128	4.99±0.22
LAN-1 ADR* >99 % MDR1+	Neuroblastoma	Adriamycin	128	4.92±0.36
LAN-1 5FU*	Neuroblastoma	5-fluorouracil	64	4.12±0.31
NB69**	Neuroblastoma	-	1	3.10±0.15
Kelly*	Neuroblastoma	-	1	5.2±0.42
SK-N-AS**	Neuroblastoma	-	1	6.3±0.21
NIH-3T3	Mouse fibroblasts	-	1	>21.00
MRC-5	Human embryonic fibroblasts	-	1	>40.00

* Cells with MYCN amplification, ** Cells without MYCN amplification

for 20 min. Supernatants (30 μg) were resolved by sodium dodecylsulfate polyacrylamide gel electrophoresis (SDS-PAGE) in a gradient gel of 4–12% (Invitrogen, Karlsruhe, Germany) using MES buffer, and transferred onto Hybond nitrocellulose paper (Amersham, Freiburg, Germany) overnight. Primary and secondary antibodies were used following the recommendations of their respective manufacturers. Antibodies were purchased as follows: anti-$p21^{Cip1}$, anti-β-actin (Sigma-Aldrich, Munich, Germany); anti-N-myc (Becton Dickinson, Krefeld, Germany); antimouse, -rat and -rabbit IgG, horseradish peroxidase (HRP)-linked whole antibody (Amersham Biosciences, Freiburg, Germany). Proteins were detected using Enhanced Chemi-Luminescence (ECL), (Amersham Biosciences, Freiburg, Germany) according to the manufacturer's instructions.

Semiquantification of DNA damage

Exponentially growing LAN-1 cells were seeded at a density of 2.5×10^6 cells / $125cm^2$-flask. After allowing 24 hrs for anchorage, cultures were exposed to concentrations from 1–20 μM of nemorosone for 6 hrs. Cells were then washed and incubated in a drug-free medium for an additional 18 hrs. Subsequently, DNA isolation was performed according to the method of Chiao [20]. 50 μg of DNA of each sample were separated on a 1.8% agarose gel for 15 hrs at 1.2 V/cm in 0.5x TRIS borat EDTA (TBE) buffer. Thereafter, the gel was stained with 0.5 μg/ml ethidium bromide for 20 min. and destained for 20 min. in distilled water. Damaged DNA (DNA 'laddering') was visualized using a standard transluminator. Semi-quantitative analyses were performed as described above, with prior incubation of the cells with 1 μCi/ml [^{14}C]-d-thymidine (Sigma-Aldrich, Munich) for 24 hrs. DNA laddering was visualized using a transluminator and the fragmentation lanes cut off, melted in 2 ml of 1N HCL at 50°C and dissolved in 10 ml of liquid scintillation cocktail (Packard, Meriden, CT, USA). The radioactivity was counted on a TPICARB 2100RT scintillation counter (Packard, Meriden, CT, USA) and reported as cpm (counts per minute).

Caspase-3-like activity

Activity of caspase-3 in cell extracts was detected using a colorimetric caspase-3 cellular activity assay kit (Calbiochem) based on cleavage of the synthetic caspase substrate-1 linked to the chromophore p-nitroanilide (Ac-DEVD-pNA). Exponentially growing cells were seeded at a density of 1.0×10^6 cells / $125cm^2$-flask. After allowing 24 hrs for anchorage, cultures were exposed to concentrations from 1 to 10 μM of nemorosone for 4 hrs. Preparation of cell extracts and analysis of caspase-3 activity was performed according to the manufacturer's protocol. The amount of hydrolyed substrate was measured as an optical density at 405 nm. The activity of caspase-3 was

expressed in arbitrary units defined as the maximal increase of optical density, derived by linear regression, per 1.0×10^6 cells for 30 min.

Cellular activation of signalling ELISA (CASE) assay

The phosphorylation status of cytosolic proteins (*e.g.* extracellular signal-regulated kinase, ERK1/2) involved in signal transduction pathways was monitored using the Cellular Activation of Signalling ELISA CASE™ Kit (SuperArray, Frederick, MD, USA). The kit is based on two antibodies, the first one recognizing the whole protein to be investigated and the second one exclusively detecting its phosphorylated form. Briefly, 2×10^3 LAN-1 cells/well were seeded in a 96-well plate and after 24 hrs, cells were treated with 2-fold their IC_{50} of nemorosone for an additional 24 hrs. The experiments were evaluated comparing the absorbance determined on an ELISA reader MRXII (Dynex, Berlin, Germany) at 450 nm using an optional reference wavelength of λ = 655 nm.

MEK1/2 activity measurement

The influence of nemorosone on the MEK1/2 kinase activity was measured using the MEK1/2 Kinase Assay Kit (New England BioLabs GmbH, Frankfurt, Germany) as described in the manufacturer's instructions. 20×10^6 untreated LAN-1 cells in exponential growth phase were used as source of activated MEK1/2 (Ser 217/221) kinase. Cells were lysed in 1x Cell Lysis Buffer (20 mM Tris pH 7.5, 150 mM NaCl, 1 mM EDTA, 1 mM EGTA, 1% Triton X-100, 2.5 mM sodium pyrophosphate, 1 mM β-glycerol phosphate, 1 mM Na3VO4, 1 µg/ml leupeptin, 1 mM PMSF). The cell lysates were incubated with phospho-MEK1/2 antibody with gentle rocking overnight at 4°C. The immunocomplexes were then obtained using protein A-sepharose CL-4B (Sigma-Aldrich, Munich, Germany) by incubation with gentle rocking for 3 hrs at 4°C. The enzymatic activity was measured as follows: precipitates were re-suspended in kinase buffer (25 mM Tris pH 7.5, 5 mM β-glycerol phosphate, 2 mM DTT, 0.1 mM Na3VO4, 10 mM MgCl2, 200 µM ATP), 2 µg of inactive p42 MAPK protein and increasing concentrations of nemorosone (1–8 µM) diluted in kinase buffer were added and incubated for 30 min. at 30°C. Finally, the phosphorylation status of MAPK was qualitatively analysed by immunoblotting as described above, employing a phospho-p44/42 MAPK (Thr202/Tyr204) monoclonal antibody.

Isobologram

The simultaneous effect of nemorosone and the Raf-1 kinase inhibitor BAY 43-9006 (gift from Dr. Dirk Strumberg, Herne, Germany) was analysed by the isobologram method (50% isodose) described by Steel and Peckham [21]. Briefly, the IC_{50} for both substances were first determined using the SRB proliferation assay. Applying fixed percentages of the IC_{50} for the first drug (20, 40, 60, 80 and 100%) and varying the concentration of the second drug from 0.1 to 50 µM, the variation in the resulting IC_{50} was determined for every percentage. The same procedure was carried out inversely for the second drug. Dose-response curves were then plotted and evaluated.

Akt/PKB activity measurement

The influence of nemorosone on the Akt/PKB kinase activity was measured using the Akt/PKB Kinase BioAssay (US Biological, Staufen, Germany) as described in the manufacturer's instructions. 30×10^6 untreated LAN-1 cells in exponential growth phase were used as source of Akt/PKB. Briefly, after immunoprecipitation of Akt/PKB, its enzymatic activity was measured as follows: precipitates were re-suspended in kinase buffer, 1 µg of GSK-3 fusion protein and 10 µl of increasing concentrations of nemorosone (2–8 µM) diluted in kinase buffer were added and incubated for 30 min at room temperature. Finally, the phosphorylation status of GSK-3 fusion protein was qualitatively analysed by immunoblotting as described above, employing the appropriate antibodies.

Statistical analysis

All data are given as means ± SEM. The comparison of means between the groups was performed by one-way analysis of variance (ANOVA) using the Bonferroni post-hoc test corrections. CASE and FACS analysis results were subjected to Student's t-test. Statistical significance was accepted when $P<0.05$. Western blots and isobologram analysis data were descriptive and were not statistically analysed.

Results

Isolation of nemorosone

With the above described method, sufficient quantities of this substance (approximately 500 mg) were produced for biochemical characterization. The structure of nemorosone was elucidated employing nuclear magnetic resonance (NMR) and mass spectroscopy (data not shown). The results of the structural analysis correspond exactly with nemorosone as published previously [16].

Determination of IC_{50} values

Previous studies described cytotoxic effects of nemorosone in various cancer cell lines [17, 22]. To initially characterize nemorosone as an anti-neuroblastoma agent, neuroblastoma cell lines NB69, Kelly, SK-N-AS, and LAN-1 (the latter comprising both parental and chemotherapy refractory sub-lines) were exposed to increasing concentrations of nemorosone for 24 hrs, whereas NIH3T3 mouse fibroblasts and MRC-5 human embryonic lung fibroblasts served as non-tumourigenic controls. As depicted in Table 1, both neuroblastoma parental cell lines and all derived chemotherapy refractory sub-lines showed IC_{50} values between 3.1±0.15 and 4.9±0.22 µM, without displaying any cross resistance to cisplatinum, etoposide, adriamycin or 5-fluorouracil. Fibroblast control cell lines showed much higher IC_{50} values (21–40 µM).

Cell cycle regulation in LAN-1 cell line

To get a first hint about the mechanisms responsible for the antitumoural effect of nemorosone, FACS-based cell cycle analyses

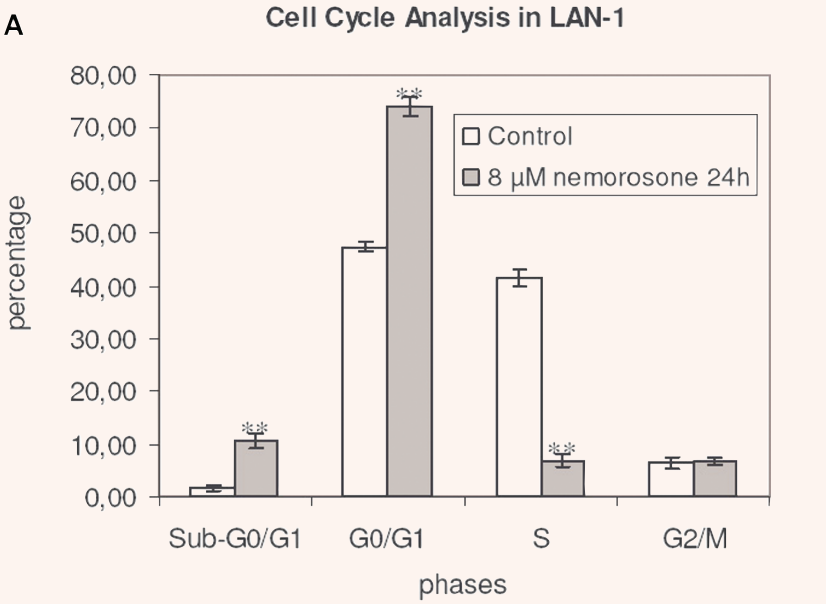

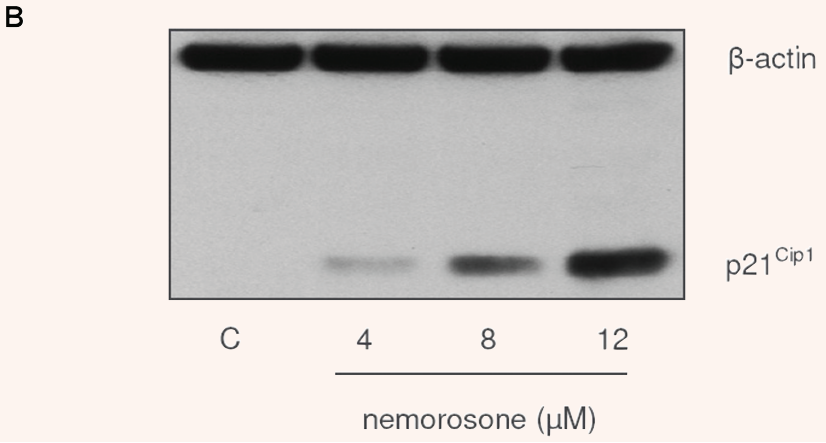

Fig. 1 Influence of nemorosone on cell cycle regulation in LAN-1. A: Cell cycle distribution of LAN-1 cells after exposure to 8 µM of nemorosone for 24 hrs. Cytometric analyses were performed using propidium iodide (PI) staining and BrdU incorporation. A highly significant increase of cells in sub-G0/G1 and G0/G1 (n = 3, $P \leq 0.001$)** phases as well as a decrease of those in S-phase (n = 3, $P \leq 0.001$)** is shown. No influence of nemorosone in the G2/M was observed (n = 3, $P \leq 0.631$). Results are represented as mean ± standard deviation of an experiment performed in triplicate. B: Influence of nemorosone on the protein level of $p21^{Cip1}$ in LAN-1 as detected by immunoblotting. Induction of $p21^{Cip1}$ after exposure to nemorosone for 24 hrs. Lane 1: control, lanes 2–4 increasing concentrations of the drug. An induction of this Cyclin-dependent Kinase Inhibitor (CDKI) is detectable after incubation with 1-fold the IC_{50} of nemorosone. The results depicted are representative for three independent experiments.

were performed. In LAN-1, 8 µM (~2-fold IC_{50}) of nemorosone increased the portion of cells in G0/G1-phase over a period of 24 hrs in a highly significant manner (n = 3, $P \leq 0.001$), while simultaneously decreasing the percentage of cells in S-phase (Fig. 1A).

To further elucidate potential mechanisms leading to G0/G1 arrest, the effect of nemorosone on the protein levels of $p21^{Cip1}$, one of the major regulatory proteins controlling the progression of the cell cycle from G1- to S-phase, was analysed. As shown in Figure 1B, increasing concentrations of this compound induced a robust up-regulation of $p21^{Cip1}$ protein levels. Thus, nemorosone-induced anti-tumoural activity may be mediated by increased expression of $p21^{Cip1}$, leading to G1 arrest.

DNA damage analysis and activation of caspase-3

Since several compounds leading to cell cycle arrest subsequently induce DNA fragmentation and apoptosis, the DNA integrity was examined after exposing LAN-1 cells to increasing concentrations of nemorosone for 6 hrs. DNA damage, a typical hallmark of late apoptosis, was observable at 5 and 10 µM in a highly significant manner (Fig. 2A). Semi-quantitative measurement of radioactive DNA extracted from [^{14}C]-d-thymidine labelled cells exposed to nemorosone further confirmed these findings (Fig. 2B). On the other hand, nemorosone was able to induce a highly significant increase of caspase-3-like activity after 4 hrs of drug-exposure (Fig. 2C). The stimulation of

caspase-3-like activity by nemorosone was dose-dependent and was comparable to the induced stimulation of these proteases by etoposide at high concentrations (10 μM).

Inhibition of Akt/PKB kinase activity by nemorosone

Although we found Akt/PKB to be phosphorylated—and thus activated—upon nemorosone treatment, this anti-apoptotic factor was apparently unable to promote cell survival. We hence analysed if this activation was possibly counterbalanced by a direct inhibitory effect of nemorosone on the enzymatic activity of Akt/PKB. Using GSK-3 fusion protein as a substrate, we found Akt/PKB kinase activity to be inhibited at concentrations starting at 0.5-fold of the IC_{50} (2 μM) in LAN-1 cells, suggesting that Akt/PKB might be one of the targets of nemorosone in the living cell (Fig. 3A).

Effect on the phosphorylation status of some key signal transducers

In order to find out whether members of the MAPK family or Akt/PKB are involved in mediating the cytotoxic activity of nemorosone in LAN-1 cells, the phosphorylation status of ERK1/2, JNK, p38 MAPK and Akt/PKB was examined using the CASE technique. After exposing the cells to nemorosone at a concentration of 8 μM for 24 hrs, a significant dephosphorylation of ERK1/2 as compared to the untreated controls was observed. Contrary to that, the modulation of the phosphorylation status on Akt/PKB, p38 MAPK and JNK were not statistically significant (Fig. 3B).

Inhibition of MEK1/2 kinase activity by nemorosone

To further investigate the mechanism for the decrease in phospho-ERK1/2 in the living cell by nemorosone, the kinase activity of MEK1/2 was examined. Nemorosone inhibited the kinase activity of MEK1/2 isolated from LAN-1 cells at concentrations as low as 8 μM, which represents twice the IC_{50} (Fig. 3C). This is congruent with the low phosphorylation status of ERK1/2 observed in the living cell, suggesting that MEK1/2 might be another physiological target of nemorosone.

Synergistic effect with a Raf-1 inhibitor

Due to the fact that nemorosone induced a dephosphorylation of ERK1/2 and a phosphorylation of Akt/PKB, we investigated if any potentiation might take place combining nemorosone with BAY 43-9006, a Raf1 inhibitor which shows a similar IC_{50} in LAN-1

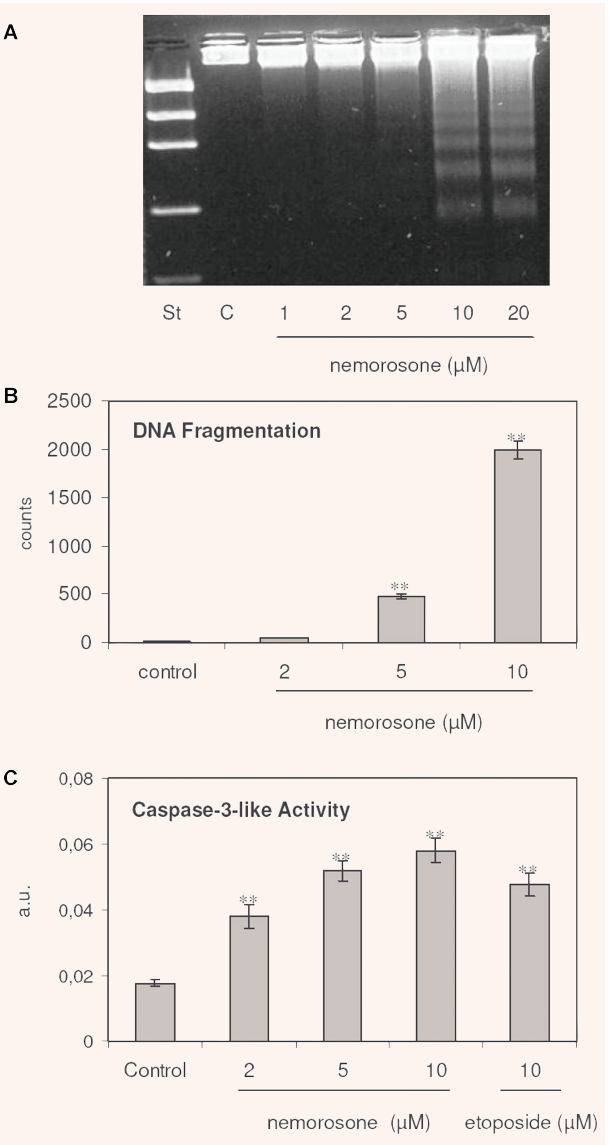

Fig. 2 Induction of apoptotic DNA strand breaks and caspase-3 activity by nemorosone in LAN-1. A: Representative results of a qualitative analysis of fragmented DNA separated on agarose gels. Lane 1: DNA standard; lane 2: control; lanes 3–7: cells incubated with increasing concentrations of nemorosone. B: Results in triplicate of a semi-quantitative DNA-double strand-breaks analysis in [^{14}C]-d-Thy-labelled LAN-1 cells induced by exposure to increasing concentrations of nemorosone for 6 hrs. Increase of DNA fragmentation is highly significant for 5 and 10 μM of the drug. C: Results in triplicate of a caspase-3-like activity measured after 4 hrs of incubation with increasing concentrations of nemorosone. Increase of caspase-3-like activity is highly significant for 2, 5 and 10 μM of the drug. Etoposide (10 μM) was added as a control. Values depicted in B and C are represented as mean ± SEM, n = 3 P<0.001**.

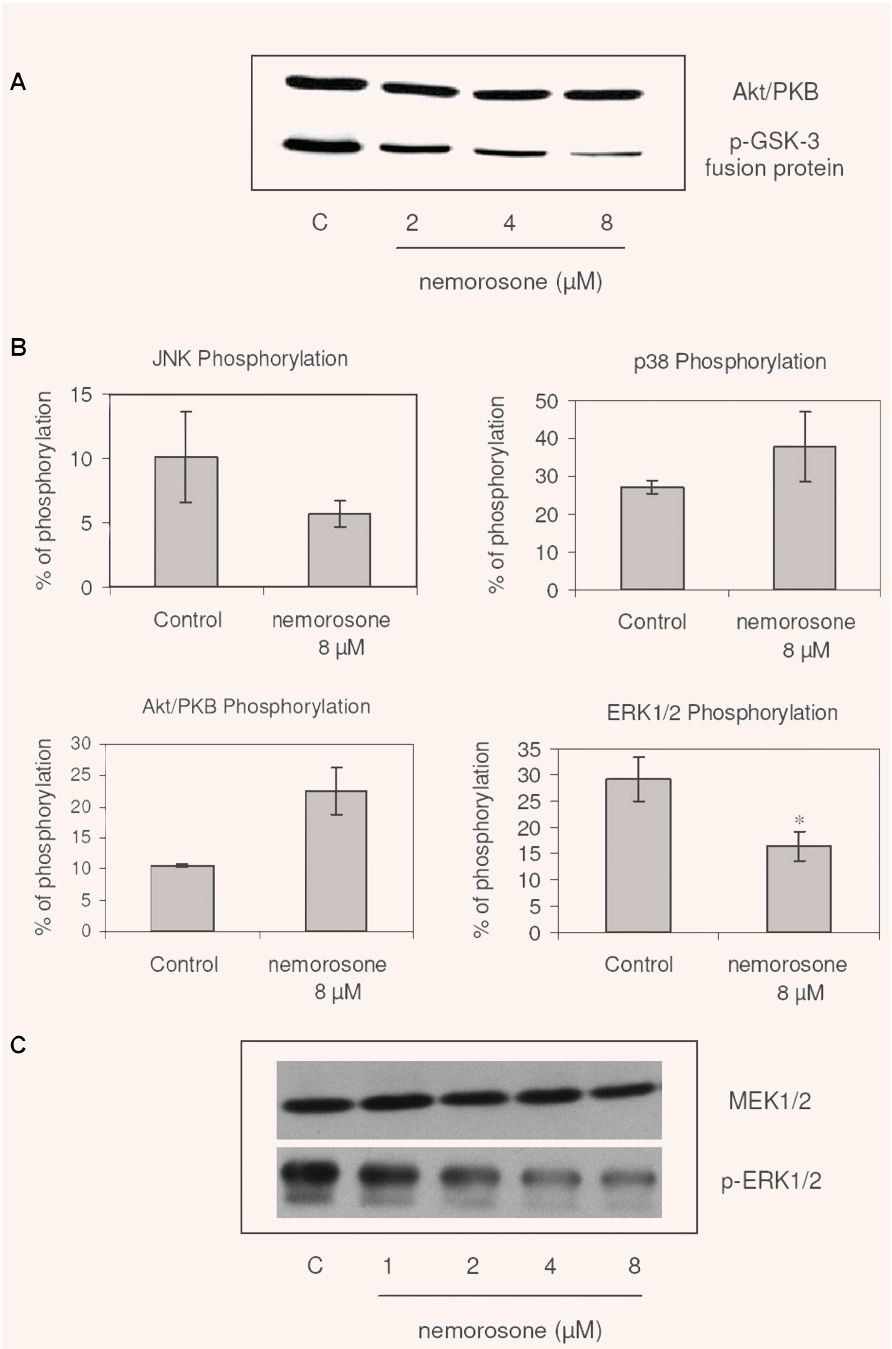

Fig. 3 Inhibition of Akt/PKB and MEK1/2 kinase activities and modulation of some transducers by nemorosone in LAN-1 cells. **A**: The influence of nemorosone on the *in vitro* activity of immunoprecipitated Akt/PKB as measured based on the phosphorylation of the glycogen synthase kinase (GSK)-3 fusion protein, was detected by immunoblotting. A marked impairment of Akt/PKB kinase activity is shown after treatment with 2 μM. Lane 1: control; lanes 2–4: nemorosone 2–8 μM. Results are representative for three independent experiments. **B**: Modulation of phosphorylation statuses as assessed by CASE assay; cells incubated with 8 μM of nemorosone for 24 hrs. No significant activation of JNK ($P = 0.281$, n = 3), p38 MAPK ($P = 0.187$, n = 3) and Akt/PKB ($P = 0.056$, n = 3) as well as a significant dephosphorylation of ERK1/2 ($P = 0.023$, n = 3)* compared to untreated controls were detected. The results depicted represent the mean ± S.D. of three independent experiments. **C**: The influence of nemorosone on the *in vitro* activity of immunoprecipitated MEK1/2 as measured based on ERK1/2 phosphorylation was detected by immunoblotting. A marked impairment of MEK1/2 kinase activity is shown after treatment with 2 μM. Lane 1: control; lanes 2–5: nemorosone 1–8 μM. Results are representative for three independent experiments.

wildtype (Fig. 4A and B). We simultaneously incubated LAN-1 cells with nemorosone and the Raf-1 inhibitor BAY 43-9006 at isobolic concentrations. As shown in Figure 4C, co-administration of both drugs yielded a synergistic effect on the IC_{50}. Thus, nemorosone could mediate its effect in part *via* the Ras/Raf/MEK/ERK pathway.

Expression of N-myc in LAN-1 cell lines

Amplification of the MYCN oncogene or overexpression of N-myc oncoprotein has been reported to be associated with chemotherapy resistance and poor prognosis in neuroblastoma. With regard

to the fact that nemorosone induced an overexpression of $p21^{Cip1}$ which is known to down-regulate N-myc, the steady-state expression of this oncoprotein was measured after exposing both parental LAN-1 and etoposide resistant ($MDR1^+$) cell lines to this compound. As depicted in Figure 5, Western blots revealed a down-regulation of N-myc protein levels. Interestingly, in LAN-1 ETO ($MDR1^+$) displaying a RF of approximately 128, this effect was comparable to the parental cell line.

Discussion

Neuroblastoma is one of the childhood tumours whose treatment suffers from high chemotherapy resistance leading to the death of more than 40% of the patients. Thus, new chemotherapeutic agents are needed which circumvent common intrinsic or acquired resistance mechanisms. A recently developed RP-HPLC strategy developed in our laboratory enabled us to purify a highly homogeneous cytotoxic compound from *Clusia rosea* resins. The structural elucidation of this compound, employing NMR and mass spectroscopy corresponds exactly to the isoprenylated benzophenone nemorosone published previously [16].

The cytotoxic effects of nemorosone on various neuroblastoma cell lines occurred in the range below 6.5 μM, while no cross-resistance in sub-lines resistant to four different chemotherapeutic agents widely employed in cancer treatment could be detected. In contrast to neuroblastoma cells, fibroblasts showed high resistance to this agent (Table 1).

Cell cycle studies revealed that nemorosone induces an accumulation of the G0/G1 fraction with a parallel reduction of S-phase fraction in LAN-1 cells (Fig. 1). Here, overexpression of $p21^{Cip1}$ might play an important role in exerting this effect, as abundant $p21^{Cip1}$ binds to the cyclin D/cyclin-dependent kinase (Cdk)4 and cyclin E/Cdk2 complexes, inhibiting their activity in the progression from G1- to S-phase [23]. The expression of $p21^{Cip1}$ is activated by p53, a major control element of cell cycle arrest and apoptosis which is activated, amongst others, in response to DNA damage [24]. To further elucidate the role of $p21^{Cip1}$ induction in the observed cell cycle arrest, functional studies will have to be performed in the future.

Apoptosis-inducing compounds specifically targeting tumour cells are expected to be ideal anti-tumour drugs, because apoptotic cell death, in contrast to necrosis, does not induce an inflammatory response. Nemorosone was found to induce DNA fragmentation, a typical hallmark of late apoptosis, in a dose-dependent manner. This small molecule seems to exert its cytotoxic effect in part *via* apoptosis induction, as the concentration inducing DNA damage was found to be as low as 5 μM (Fig. 2A and B). Consistent with this finding, we detected an induction of caspase-3-like activity by nemorosone in a drug-concentration dependent manner (Fig. 2C). Changes in both DNA fragmentation and caspase-3-like activity were statistically highly significant.

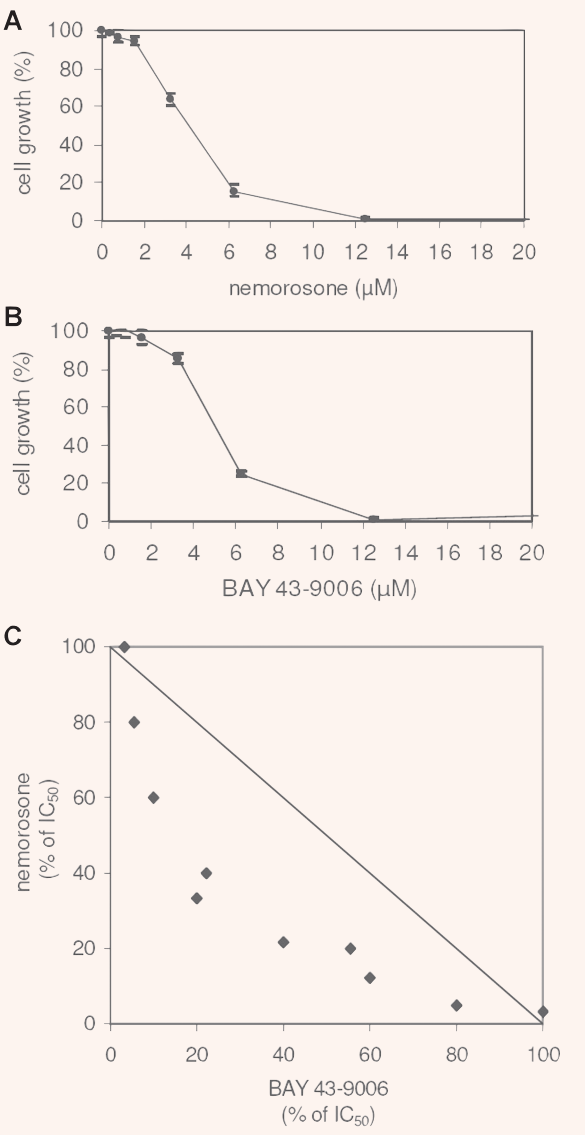

Fig. 4 Isobologram resulting from the simultaneous incubation of LAN-1 with nemorosone and the Raf-1 inhibitor BAY 43-9006. **A** and **B**: Cytotoxicity dose–response curves of nemorosone and BAY 43-9006, respectively in LAN-1 wild-type. **C**: Measurement of cytotoxicity in LAN-1 after simultaneous incubation with these two compounds for 24 hrs. A synergistic effect is shown. The diagrams depicted are representative for three independent experiments.

Moreover, DNA damage can be stimulated, amongst others, via inhibition of topoisomerases I and II, which upon formation of a putative cleavage complex with the DNA triggers its degradation [25]. Complete inhibition of the enzymatic activity of topoisomerases by nemorosone was achieved only at a concentration of 100 μM, which represents more than 20-fold the IC_{50} in the

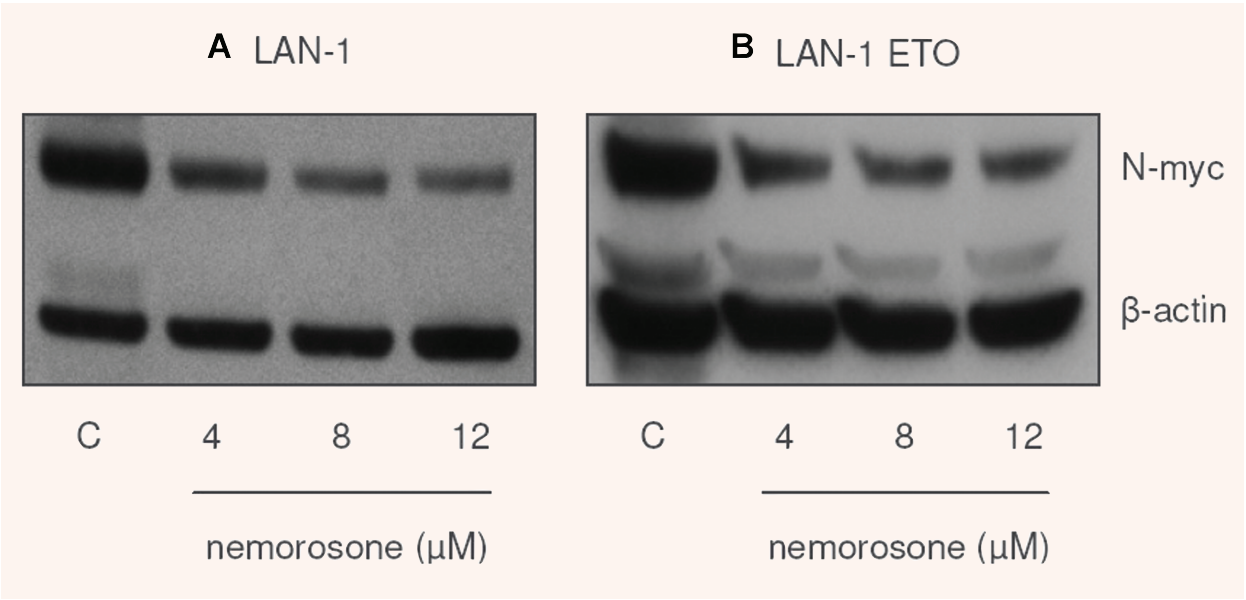

Fig. 5 Influence of nemorosone on the protein level of N-myc in LAN-1 and LAN-1 ETO. Down-regulation of N-myc in **A**: LAN-1 and **B**: LAN-1 ETO ($MDR1^+$) neuroblastoma cell lines by incubation with increasing concentrations of nemorosone for 24 hrs. Lane 1: control, lanes 2–4: nemorosone 4–12 μM. Results are representative for three independent experiments.

examined cell lines. These findings do not support the primary activity of nemorosone as being a topoisomerase inhibitor (data not shown). The fact that fibroblasts, which generally do not display telomerase activity [26], were highly resistant to nemorosone lead us to the strategy to further focus on the examination of telomerase as a possible target. But since complete inhibition of telomerase activity only occurred at 10-fold the IC_{50} of nemorosone in LAN-1 cells, this enzyme, like the topoisomerases, was not taken into consideration as a physiological target (data not shown).

In order to elucidate how nemorosone modulates particular signal transducers at concentrations of up to 2-fold the IC_{50} in the living cell, its impact on the phosphorylation status of key regulatory elements of some signal transduction pathways was investigated. As shown in Figure 3B, nemorosone treatment decreased the phosphorylation status of ERK1/2 significantly, while no relevant modulation of JNK, p38 MAPK and Akt/PKB was observed.

We conclude that the inhibition of MEK1/2 (Fig. 3C) might be the primary cause for the significant dephosphorylation of ERK1/2. As a secondary explanation, MAPK phosphatases (MKPs) might be activated through the exposure of LAN-1 cells to nemorosone, since there are specific MKPs that act negatively on ERK1/2 and JNK phosphorylation, respectively [27].

On the other hand, the slightly increased phosphorylation status of Akt/PKB could result from the stimulation of its upstream activators like integrin-linked kinase (ILK), 3-phosphoinositide-dependent protein kinase 1 (PDK-1) or DNA-protein kinase (DNA-PK), the latter being also stimulated by caspase-3 activity, resulting in DNA damage as discussed above [28].

Nemorosone works synergistically with BAY 43-9006 (Fig. 4C), an inhibitor of Raf-1 which acts upstream of ERK1/2. Thus, we assume that the simultaneous application of the two drugs targets the Ras/Raf/MEK/ERK kinase pathway at different points.

It is well known that ERK1/2 directly activates MYCN transcription. Nemorosone induces a drastic drug-dependent down-regulation of N-myc protein levels. We therefore expect that many target genes that depend on MYCN activation might be repressed through the action of this compound. Consequently, the inhibition of ERK1/2 phosphorylation by nemorosone seems to be at least in part responsible for the down-regulation of N-myc in LAN-1 and LAN-1 ETO ($MDR1^+$) cells (Fig. 5).

Nemorosone induced a slight phosphorylation of Akt/PKB, an effect which is normally associated with an increase of its kinase activity. In contrast, this substance inhibited the kinase activity of immunoprecipitated Akt/PKB *in vitro* as measured by its ability to phosphorylate GSK-3 fusion protein, suggesting Akt/PKB to be one of the molecular targets of this compound (Fig. 3A). We speculate that the inhibition of Akt/PKB might lead to a rescue reaction of the cell trying to circumvent the inhibition of Akt/PBK by enforcing its phosphorylation or *via* DNA-PK activation.

GSK-3β, a key inhibitor in Wnt/β-catenin signalling, is consequently activated *via* Akt/PKB inhibition. As a result, it is expected that genes governed by this pathway, among which N-myc and

cyclin D can be found, will be repressed if Akt/PKB is inhibited, conferring a strong anti-proliferative effect [10].

The fact that nemorosone is a modulator or inhibitor of MEK1/2 and Akt/PKB cascades makes it a potential candidate for specific molecular therapy, as these pathways exert cardinal functions in the transduction and integration of extracellular and intracellular oncogenic signals. Blockage of these pathways results in growth inhibition and apoptosis of tumours [29, 30].

Moreover, we were able to confirm the results related to the mechanisms of action of nemorosone in other neuroblastoma cell lines studied in our laboratory (NB69, Kelly, SK-N-AS; data not shown).

An interesting phenomenon is the low cytotoxicity of nemorosone in non-tumoral cell lines. This intriguing finding is currently under investigation in our laboratory. It has been described that fibroblasts express both ERK1/2 and Akt/PKB signal transducers [31]. Thus, if the proposed mechanisms of action *via* ERK1/2 and/or Akt/PKB mediate cytotoxicity in neuroblastoma cells, the reason why fibroblasts are resistant to nemorosone treatment, although expressing both proteins, remains unclear. Additionally, should be to explain if the resistance of fibroblasts to nemorosone corresponds to differences in the DNA repair mechanisms, differential metabolic pathways and/or drug uptake in comparison to the cancer cells analysed. In this context, the role of glutathione for the detoxification mechanisms in the fibroblasts, neuroblastoma and neuroblastoma MDR1$^+$ sub-lines will be studied in the future. It is expected that the nemorosone mediated inhibition of ERK1/2 and the putative Akt/PKB inhibition will affect global gene expression in the cell in a tissue-dependent manner [32]. Other mechanisms of action have been proposed for different polyisoprenylated benzophenone representatives such as the inhibition of histone acetyltransferase by garcinol [33].

Taken together, in order to propose a tentative primary target which could explain the mechanisms of action of nemorosone, we only took into consideration those biochemical processes or cellular elements that are affected by near to 3-fold or less the IC_{50} in neuroblastoma cells. Following this premise, we propose that the cytotoxicity of nemorosone possibly acts *via* inhibition of the kinase activity of one or more of the upstream elements of ERK1/2, and/or acts on different pathways, in particular the Akt/PKB cascade.

Acknowledgements

Special thanks to Dr. Angelika Eggert from the Children's Hospital Oncology Division of Duisburg-Essen University for providing us the parental cell lines, and Mr. Heinz Bandmann for his excellent assistance with the NMR studies. We also thank the West German Cancer Center their help provided in this investigation. This investigation was supported by the Katholischer Akademischer Ausländer-Dienst (KAAD), IFORES Scientific Programme of Essen University (107-05760), the West German Cancer Center and the Mildred Scheel Foundation (106993).

References

1. **Maris JM, Hogarty MD, Bagatell R, Cohn SL.** Neuroblastoma. *Lancet.* 2007; 23: 2106–20.
2. **Brodeur GM, Maris JM, Yamashiro DJ, Hogarty MD, White PS.** Biology and genetics of human neuroblastomas. *J Pediatr Hematol Oncol.* 1997; 19: 93–101.
3. **Vandesompele J, Michels E, De Preter K, Menten B, Schramm A, Eggert A, Ambros PF, Combaret V, Francotte N, Antonacci F, De Paepe A, Laureys G, Speleman F, Van Roy N.** Identification of 2 putative critical segments of 17q gain in neuroblastoma through integrative genomics. *Int J Cancer.* 2007; 122: 1177–82.
4. **Schwab M.** Molecular cytogenetics of human neuroblastoma. *Biochim Biophys Acta.* 1992; 1114: 43–50.
5. **Wenzel A, Schwab M.** The mycN/max protein complex in neuroblastoma. Short review. *Eur J Cancer.* 1995; 31A: 516–29.
6. **Cole MD, McMahon SB.** The Myc oncoprotein: a critical evaluation of transactivation and target gene regulation. *Oncogene.* 1999; 18: 2916–24.
7. **Boon K, Caron HN, van Asperen R, Valentijn L, Hermus MC, van Sluis P, Roobeek I, Weisl, Voûte PA, Schwab M, Versteeg R.** N-myc enhances the expression of a large set of genes functioning in ribosome biogenesis and protein synthesis. *EMBO J.* 2001; 20: 1383–93.
8. **Raetz EA, Kim MK, Moos P, Carlson M, Bruggers C, Hooper DK, Foot L, Liu T, Seeger R, Carroll WL.** Identification of genes that are regulated transcriptionally by Myc in childhood tumors. *Cancer.* 2003; 98: 841–53.
9. **Vivanco I, Sawyers CL.** The phosphatidylinositol 3-Kinase AKT pathway in human cancer. *Nat Rev Cancer.* 2002; 2:489–501.
10. **Shu W, Guttentag S, Wang Z, Andl T, Ballard P, Lu MM Piccolo S, Birchmeier W, Whitsett JA, Millar SE, Morrisey EE.** Wnt/beta-catenin signaling acts upstream of N-myc, BMP4, and FGF signaling to regulate proximal-distal patterning in the lung. *Dev Biol.* 2005; 283: 226–39.
11. **Li Z, Zhang J, Liu Z, Woo CW, Thiele CJ.** Downregulation of Bim by brain-derived neurotrophic factor activation of TrkB protects neuroblastoma cells from paclitaxel but not etoposide or cisplatin-induced cell death. *Cell Death Differ.* 2007; 14: 318–26.
12. **Sugimoto T, Kuroda H, Horii Y, Moritake H, Tanaka T, Hattori S.** Signal transduction pathways through TRK-A and TRK-B receptors in human neuroblastoma cells. *Jpn J Cancer Res.* 2001; 92: 152–60.
13. **Patapoutian A, Reichardt LF.** Trk receptors: mediators of neurotrophin action. *Curr Opin Neurobiol.* 2001; 11: 272–80.
14. **Takahashi-Yanaga F, Shiraishi F, Hirata M, Miwa Y, Morimoto S, Sasaguri T.** Glycogen synthase kinase-3beta is tyrosine-phosphorylated by MEK1 in human skin fibroblasts. *Biochem Biophys Res Commun.* 2004; 316: 411–25.
15. **Shira Yaari, Jasmine Jacob-Hirsch, Ninette Amariglio, Ronit Haklai, Gideon Rechavi, Yoel Kloog.** Disruption of Cooperation Between Ras and MycN in Human Neuroblastoma Cells Promotes Growth Arrest. *Clin Cancer Res.* 2005; 11: 4321–30.
16. **Cuesta-Rubio O, Velez-Castro H, Frontana-Uribe BA, Cardenas J.** Nemorosone, the major constituent of floral resins of Clusia rosea. *Phytochemistry.* 2001; 57: 279–83.
17. **Diaz-Carballo D, Seeber S, Strumberg D, Hilger RA.** Novel antitumoral compound

isolated from Clusia rosea. *Int J Clin Pharmacol Ther.* 2003; 41: 622–33.

18. **Skehan P, Storeng R, Scudiero D, Monks A, McMahon J, Vistica D, Warren JT, Bokesch H, Kenney S, Boyd MR.** New colorimetric cytotoxicity assay for anticancer-drug screening. *J Natl Cancer Inst.* 1990; 82: 1107–12.
19. **Tsugita M, Tsuru S, Takasaki T, Shinomiya N, Kobayashi S, Hanyu F.** Flowcytometric measurement of the cell cycle of experimental tumors: some devices for accurate measurement of proliferative activity. *Oncology.* 1991; 48: 343–56.
20. **Chiao C, Carothers AM, Grunberger D, Solomon G, Preston GA, Barrett JC.** Apoptosis and altered redox state induced by caffeic acid phenethyl ester (CAPE) in transformed rat fibroblast cells. *Cancer Res.* 1995; 55: 3576–83.
21. **Steel GG, Peckham MJ.** Exploitable mechanisms in combined radiotherapy-chemotherapy: the concept of additivity. *Int J Radiat Oncol, Biol Phys.* 1979; 5: 85–91.
22. **Cuesta-Rubio O, Frontana-Uribe BA, Ramirez-Apan T, Cardenas J.** Polyisoprenylated benzophenones in Cuban propolis; biological activity of nemorosone. *Z Naturforsch.* 2002; 57: 372–8.
23. **Bottazzi ME, Zhu X, Bohmer RM, Assoian RK.** Regulation of p21(cip1) expression by growth factors and the extracellular matrix reveals a role for transient ERK activity in G1 phase. *J Cell Biol.* 1999; 146: 1255–64.
24. **Kuwano K, Hagimoto N, Nomoto Y, Kawasaki M, Kunitake R, Fujita M, Miyazaki H, Hara N.** p53 and p21 ($Waf1/^{Cip1}$) mRNA expression associated with DNA damage and repair in acute immune complex alveolitis in mice. *Lab Invest.* 1997; 76: 161–9.
25. **Hong G, Kreuzer KN.** An antitumor drug-induced topoisomerase cleavage complex blocks a bacteriophage T4 replication fork *in vivo*. *Mol Cell Biol.* 2000; 20: 594–603.
26. **Meyerson M.** Role of telomerase in normal and cancer cells. *J Clin Oncol.* 2000; 18: 2626–34.
27. **Camps M., Nichols A, Arkinstall S.** Dual specificity phosphatases: a gene family for control of MAP kinase function. *Faseb J.* 2000; 14: 6–16.
28. **Durocher D, Jackson SP.** DNA-PK, ATM and ATR as sensors of DNA damage: variations on a theme? *Curr Opin Cell Biol.* 2001; 13: 225–31.
29. **Cheng JQ, Lindsley CW, Cheng GZ, Yang H, Nicosia SV.** The Akt/PKB pathway: molecular target for cancer drug discovery. *Oncogene.* 2005; 24: 7482–92.
30. **Wallace EM, Lyssikatos JP, Yeh T, Winkler JD, Koch K.** Progress towards therapeutic small molecule MEK inhibitors for use in cancer therapy. *Curr Top Med Chem.* 2005; 5: 215–29.
31. **Tong L, Smyth D, Kerr C, Catterall J, Richards CD.** Mitogen-activated protein kinases Erk1/2 and p38 are required for maximal regulation of TIMP-1 by oncostatin M in murine fibroblasts. *Cell Signal.* 2004; 16: 1123–32.
32. **Boyd KE Farnham PJ.** Identification of target genes of oncogenic transcription factors. *Proc Soc Exp Biol Med.* 1999; 222: 9–28.
33. **Balasubramanyam K, Altaf M, Varier RA, Swaminathan V, Ravindran A, Sadhale PP, Kundu TK.** Polyisoprenylated benzophenone, garcinol, a natural histone acetyltransferase inhibitor, represses chromatin transcription and alters global gene expression. *J Biol Chem.* 2004; 279: 33716–26.